

## Ultrahigh-vacuum furnace for sintering studies of ultrafine ceramic particles

John E. Bonevich, Mao-Hua Teng, D. Lynn Johnson, and Laurence D. Marks

Citation: *Review of Scientific Instruments* **62**, 3061 (1991); doi: 10.1063/1.1142154

View online: <http://dx.doi.org/10.1063/1.1142154>

View Table of Contents: <http://scitation.aip.org/content/aip/journal/rsi/62/12?ver=pdfcov>

Published by the [AIP Publishing](#)

---

### Articles you may be interested in

[An ultrahigh-vacuum system for STM studies](#)

*Rev. Sci. Instrum.* **65**, 2523 (1994); 10.1063/1.1144645

[Ultrahigh-vacuum manipulator for LEED studies](#)

*Rev. Sci. Instrum.* **45**, 1611 (1974); 10.1063/1.1686575

[Apparatus for Ultrahigh-Vacuum In Situ Thin-Film Studies](#)

*J. Vac. Sci. Technol.* **7**, 607 (1970); 10.1116/1.1315887

[A Study of Thermal Transpiration Using Ultrahigh-Vacuum Techniques](#)

*J. Vac. Sci. Technol.* **2**, 182 (1965); 10.1116/1.1492423

[Ultrahigh-Vacuum Valve](#)

*Rev. Sci. Instrum.* **30**, 944 (1959); 10.1063/1.1716395

---

**œerlikon**  
leybold vacuum

online shop  
now available  
in 12 countries



Vacuum Technology Made Easy

[www.leyboldvacuum-shop.com](http://www.leyboldvacuum-shop.com)

# Ultrahigh-vacuum furnace for sintering studies of ultrafine ceramic particles

John E. Bonevich, Mao-Hua Teng, D. Lynn Johnson,  
and Laurence D. Marks

*Northwestern University, Department of Materials Science and Engineering, 2145 Sheridan Road,  
Evanston, Illinois 60208*

(Received 20 June 1991; accepted for publication 25 August 1991)

An ultrahigh-vacuum (UHV) furnace has been designed and constructed for the purpose of investigating the sintering behavior of ultrafine ceramic particles. The UHV furnace has three main chambers for particle production, sintering, and collection with additional facilities for an UHV transfer system. The furnace system achieves a base pressure of  $4 \times 10^{-7}$  Pa through the use of turbomolecular and ion pumps. The ultrafine particles of aluminum oxide are produced by the arc discharge method resulting in the formation of highly faceted particles in the size range of 20–50 nm. The particles are then carried into the tube furnace by a flowing gas stream where they sinter at elevated temperatures. The sintered samples are collected onto a specimen cartridge which is then transported under vacuum conditions to an UHV high-resolution electron microscope for structural characterization. The unique feature of this UHV furnace system is that one is able to perform sintering studies in a clean environment thereby minimizing the influence of contaminating species on the sintering behavior.

## I. INTRODUCTION

The study of nanophase materials has been of considerable interest, given that they possess both improved mechanical behavior over bulk materials and the potential for new structures with novel properties. Yet while these materials have been studied in terms of their mechanical behavior,<sup>1–5</sup> little is known of their structure on the atomic scale, in particular the structure of the interface between particles that exist in a consolidated material. The reasons for the lack of information may be due to the fact that nanocrystalline samples prepared for microstructural characterization, e.g., in an electron microscope, have many overlapping grains which may complicate a unique interpretation. Furthermore, the process of sample preparation could, in fact, change the nature of the interfacial structure. For example, the frequently used dimpling and jet thinning techniques in electron microscopy can produce undesirable defects in the sample.

An additional factor that can have dramatic effects on the structure is contamination. The sample preparation process exposes the specimen not only to the atmosphere but also to a whole host of complicated steps, any one of which could introduce unwanted impurities. The large surface-to-volume ratios found in these materials and the fact that many properties are surface controlled mandates that the extrinsic effects of impurities be carefully scrutinized. The role of contamination is best exemplified by considering that there is considerable debate over whether the Hall–Petch<sup>6,7</sup> relation can be extended down to grain sizes typically found in nanocrystalline materials. Neiman and co-workers<sup>3,4</sup> have reported that nanocrystalline Cu and Pd samples exhibit improved mechanical behavior and that no appreciable grain-boundary diffusional creep was observed. However, Chokshi *et al.*<sup>2</sup> have contradictory evi-

dence in nanocrystalline Cu and Pd reporting a negative Hall–Petch relationship and substantial diffusional creep resulting in grain-boundary sliding.

Contamination is almost certainly the defining factor in the discrepancy between these results since the materials systems are the same, and the samples are presumably prepared and tested in a similar manner. The impurities in these systems may act to either “embrittle” or “lubricate” the grain boundaries; i.e., the behavior is controlled by extrinsic properties.

The existence of impurities can also have a dramatic effect on the thermodynamics of surfaces and the rates of surface diffusion.<sup>8</sup> For example, adsorption on surfaces might result in a negative surface stress.<sup>9</sup> Minimizing contamination is very important to the study of the virgin surfaces of alumina which act catalytically in the atmosphere, i.e., surfaces of alumina are dependent on the environment<sup>10</sup> and they act as a “getter” for oils and other hydrocarbons.

We have endeavored to investigate the atomic and interfacial structure of ceramic materials in the ultrafine particle (UFP) size range (20–50 nm) as a function of the sintering treatment. As the surface-to-volume ratio in these materials is rather large, we have also made a concerted effort to minimize the effects of impurities by conducting our experiments in an ultrahigh-vacuum (UHV) furnace where the formation and sintering processes occur in a clean environment. Furthermore, the furnace system has the capability to collect and transport the sintered samples to an UHV high-resolution electron microscope (HREM) for structural characterization. The present system represents an improvement of several orders of magnitude in cleanliness and vacuum over previous efforts. However, while we have greater control over impurities, we can not state conclusively that all contamination issues have been

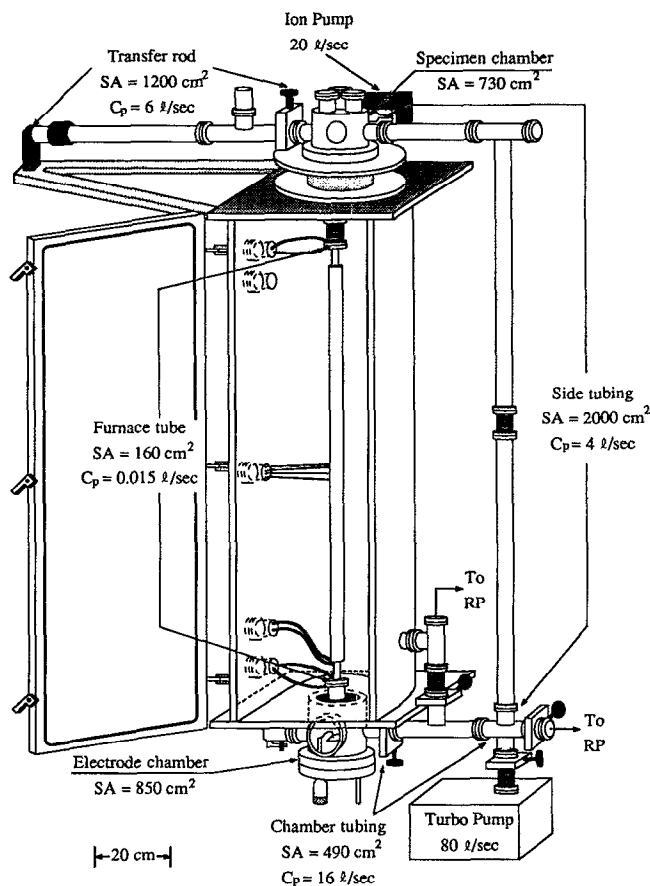


FIG. 1. Schematic diagram of the UHV furnace system. The furnace tube can be seen contained within the large furnace chamber which has its O-ring sealed door opened. The turbo and ion pumps are labeled along with the conductances and surface areas of the different chambers. The arc discharge apparatus can be seen through the viewport of the production chamber. At the top is the collection chamber with the transfer system attached. During sintering experiments the oxidizing gas is admitted, forced to flow up the furnace tube to the collection chamber, and then flows down the side tubing to exit the system through the rotary pump (RP). The whole furnace system rests upon an angle iron framework, not shown.

resolved. We present here the design details of the UHV furnace and also outline the procedures required to produce and collect sintered specimens.

## II. THE UHV FURNACE SYSTEM

The UHV furnace system has three main chambers for particle production, sintering, and specimen collection (see Fig. 1). The former and latter are simple UHV chambers, whereas the sintering process occurs in a flowing gas furnace tube which connects the production and collection chambers. In this way, the furnace system allows for sintering experiments to be a continuous process whereby the UFPs are formed in the production chamber where they aggregate into short chainlike clusters, forced to flow through the furnace tube, and are quenched and then collected for examination without any exposure to the ambient atmosphere or contaminating species.

The UFPs are produced by the arc discharge method whereby an arc is created between high-purity metal (aluminum) electrodes, in a wire and plate configuration, in an oxidizing atmosphere (Ar-20% O<sub>2</sub>). This method was used by Iijima<sup>11</sup> and Warble<sup>12</sup> to prepare powders of aluminum oxides. However, in these previous studies the UFP samples were exposed to the ambient atmosphere, either during transport to the electron microscope or during the sintering process.

In the present system, the UFP production chamber is designed so that the entire electrode configuration is confined to a single flange (see Fig. 2). The flange contains the electrical feedthroughs, a high-pressure convectron gauge (Granville-Phillips), and a rotary feedthrough for the manipulation of the wire electrode. The advantage of this system is that the electrode configuration is fixed and new material can be supplied while only one UHV seal need be replaced. The remainder of the production chamber consists of an ionization gauge and a Varian leak valve inlet for the gas mixture. The ionization gauge can be isolated from the production chamber by a butterfly valve; this eliminates arcing problems caused when the UFPs fill the chamber before rising to the furnace. In the furnace system, control of the purity of the Ar-20%O<sub>2</sub> arcing gas is very important since the alumina UFPs "see" these gases from their inception. At present, the high-purity arcing gases are delivered to the system at a line pressure of 136 kPa and are blended by flow meters individually calibrated for their respective gases. Then the mixture is fed into the leak valve which is equipped with a particulate filter.

The furnace used in the present system consists of a 91.5-cm-long sintered tube of 99.8% alumina (McDaniel Corp.) with inner and outer diameters of 0.5 and 1.1 cm, respectively. This represents a compromise between the need to adequately collimate the stream of sintered clusters and, at the same time, allow adequate evacuation of the tube. Stainless-steel sleeves are brazed onto the ends of the tube, and UHV knife-edge flanges are welded to these so that the total length of the furnace is 98 cm. The Kovar braze material (Ceramasal) must be kept below  $\approx 700^\circ\text{C}$  to maintain vacuum integrity, so the flanges are water cooled and the heated zone terminates 5 cm from the braze junctions. The furnace heat zone is a noninductive winding of 0.1-cm Mo wire along the central 80 cm of the tube. The Mo wire is encased in alumina cement and four type-R (Pt/Pt-13%Rh) thermocouples are attached at 15-cm intervals. The furnace tube is surrounded by three concentric radiative heat shields made of Mo foil. Figure 3 shows the temperature profile of the furnace tube across the heat zone.

The furnace tube is surrounded by a large vacuum chamber that has flanges for feedthroughs. These ports include an electrical feedthrough for the Mo heat winding, two water feedthroughs to cool the top and bottom flanges, and 8-pin feedthrough made of extension wire for the thermocouples, a forming gas (N<sub>2</sub>-10% H<sub>2</sub>) inlet valve, a pumping port, and sapphire viewport in the door for an optical pyrometer. This vacuum chamber, constructed for Northwestern University by Ability Engineering,<sup>13</sup> also

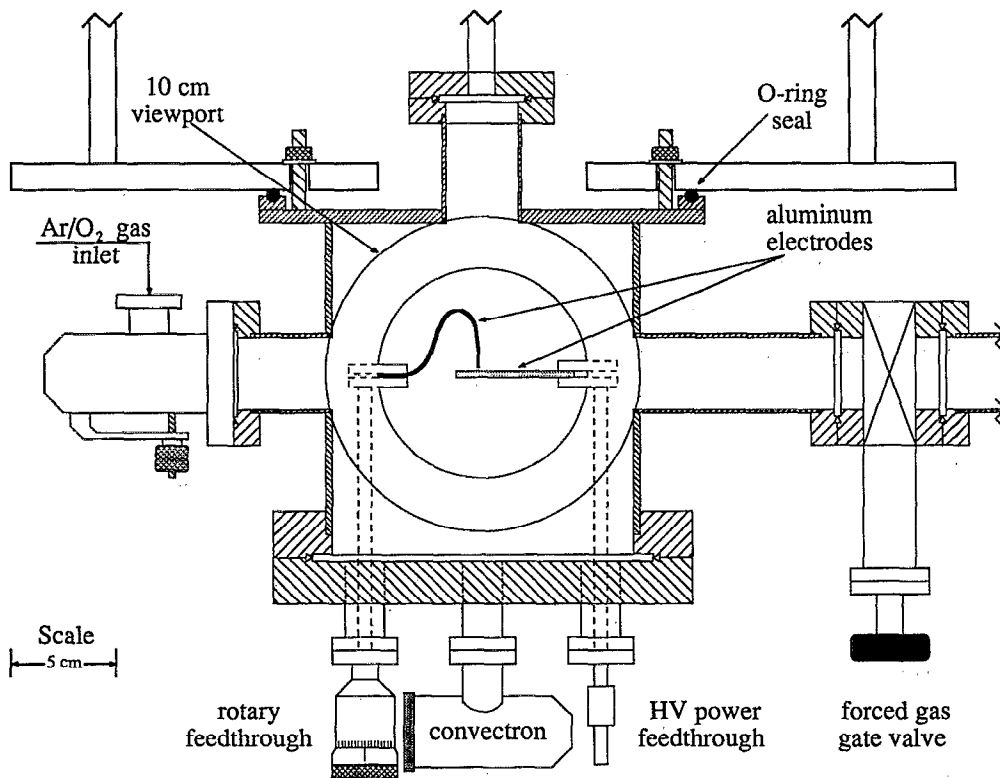


FIG. 2. Diagram of the particle production chamber. The electrode assembly (20-cm knife-edge flange) is shown containing the power and rotary feedthroughs and the high-pressure vacuum gauge. The gate valve on the right-hand side is closed during particle production to force the arcing gas (coming from the leak valve on the left-hand side) up the furnace tube for sintering experiments. The production chamber is attached to the large furnace chamber and is sealed there by an O-ring.

has 10-cm holes in the center of the top and bottom plates for the attachment of the particle production and collection chambers. The chamber is sealed by means of O-rings for the door and the top and bottom chambers; the feedthrough ports have knife-edge seals. The chamber is pumped down simultaneously with the UHV chambers to

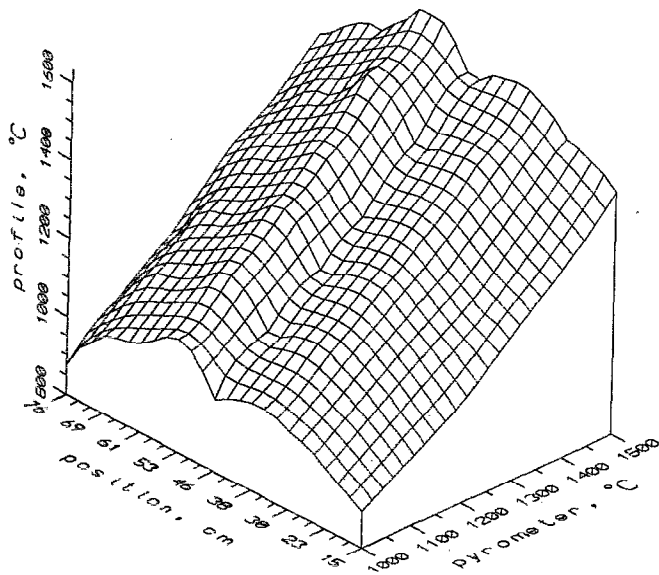


FIG. 3. Plot of the internal furnace temperature profile with distance from the top flange of the tube as a function of the temperature at the tube center as measured by an optical pyrometer. The Mo heat shields at the tube center have holes for the optical pyrometer and the external thermocouples. This hole in the heat shields allows some heat loss resulting in the temperature dip at the tube center.

minimize any pressure differential across the furnace bellows. However, the chamber is only connected to a rotary pump and is maintained at about 1 Pa at all times with the exception of particle production when the pressure is increased, in conjunction with the production chamber, to 6–10 kPa.

The furnace tube is connected to the particle production and collection chambers in order to achieve UHV conditions and to isolate the heating elements and UHV chambers during particle production. This isolation is necessary because when the furnace is in operation, the Mo windings and heat shields must be kept in a reducing atmosphere, i.e., the  $N_2$ -10%  $H_2$  forming gas. However, the UFPs of interest are created in an oxidizing atmosphere of Ar-20%  $O_2$ . The incompatibility of these two requirements demands isolation seals of the highest integrity, for if these seals should fail the results would be catastrophic.

In the current design configuration the furnace tube is rigidly connected to the flange of the particle production chamber which protrudes through the 10-cm hole in the bottom plate of the furnace chamber. The connection of the Mo winding leads and the lower cooling lines are also made at the bottom of the furnace chamber. This allows the top of the furnace tube to be "free floating" in order to accommodate the thermal expansion of the tube and also to minimize any bending moments upon the tube that would result in the breaking of the seals or the tube itself. It should be noted, however, that the thermocouples are physically attached at the center of the tube and that the top flange has cooling lines connected to it. The obstacles these connections pose to the free motion of the tube are circumvented by providing slack in the case of the thermo-

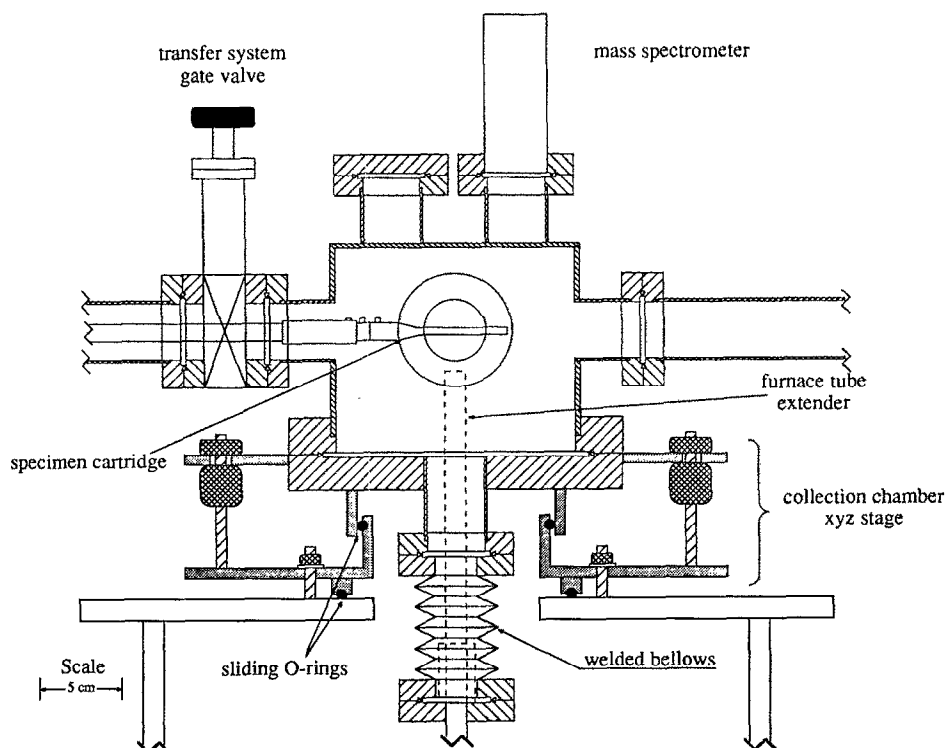


FIG. 4. The specimen collection chamber is attached to the top of the furnace chamber. Here the xyz stage is shown that allows the chamber to be positioned above the furnace tube so that any bending moments on the tube are minimized. The xyz stage has sliding O-ring seals to allow for this position adjustment. The specimen cartridge is shown positioned above the furnace tube extender which freely floats with the thermal expansion of the furnace. The thermal expansion is accommodated by the welded bellows. The specimen cartridge can be retracted after collection, its gate valve sealed, and the transfer system moved to the UHV electron microscope for structural characterization.

couples and using a wide radius cooling line, made of lightweight flexible tubing, that encircles the top flange.

The connection between the particle collection chamber and the furnace tube is accomplished by means of a flexible bellows which, in addition to minimizing any bending moments on the tube, allows the tube to expand and contract freely during a temperature cycle (the tube expands by  $\approx 1.4$  cm at  $1500^\circ\text{C}$ ). The collection chamber is attached to a specimen stage that, by means of sliding O-rings, allows for three degrees of freedom (see Fig. 4). Thus, the particle collection chamber and flexible bellows can be aligned as perfectly as possible with the furnace tube so that the combination functions cooperatively. As a result of this system, however, there exists a gap of 22 cm between the exit hole of the furnace and the microscope specimen cartridge where the particles are to be collected. To minimize any spread of the particle stream and also avoid the high surface area of the bellows, a tube extender is placed in the gap. The extender, constructed from the same alumina material as the furnace tube with a wide base to provide stability, rests upon the top flange of the furnace tube and terminates a short distance below the height of the specimen cartridge. The extender is allowed to rise and fall in conjunction with the furnace tube; however, it does not reach the high temperatures that exist within the furnace. The distance between the exit of the extender and the specimen cartridge therefore varies from 10 mm at  $1000^\circ\text{C}$  to 7–8 mm at  $1200^\circ\text{C}$ . The short distance ensures that nearly all of the particles produced pass by the specimen cartridge with very minimal losses to the chamber walls or the bellows.

The microscope grid (holey SiO film on a copper mesh) on which the sintered clusters are collected is held

in a microscope cartridge. This cartridge is manipulated by a rotary/linear magnetically coupled feedthrough to allow for the exact positioning of the cartridge directly in the UFP/oxidizing gas stream. The positioning of the cartridge is facilitated by two viewports in the collection region to ensure exact alignment; the importance of this feature is that the microscope grid presents only a 1-mm cross section to the particle stream and the particles of interest are those that travel along the central axis of the furnace tube. If a wider cross section is desired, however, the specimen holder can be replaced with one designed (by JEB) for 3-mm holey grids.

The electron microscope specimen cartridge, connected to the rotary/linear feedthrough, can be retracted fully from the collection chamber. Once retracted into the portable transfer system (PTS), the specimen can be isolated from the rest of the vacuum system by a gate valve. If so desired, the isolated region can be pumped by a small battery-powered 1-l/s ion pump. The PTS concept is that once the specimen has been collected, it can be transferred to the UHV-H9000 electron microscope under high vacuum. A pressure of  $10^{-6}$  Pa is attainable within 1 h of collection; UHV is achieved by baking the entire system. The PTS ensures that specimens are not exposed to contamination from the atmosphere or residual gases during transfer to the UHV microscope.

### III. UHV FURNACE CONDUCTANCE ANALYSIS

The ultimate obtainable pressure can be estimated by analyzing the conductance of the furnace system. Figure 1 shows the surface areas of each of the components, which total approximately  $6300\text{ cm}^2$ . The conductances for the

tubing can be calculated by the standard equation for molecular flow (pressures below 0.1 Pa),

$$C_p = 11.6(D^3/L) \text{ l/s}, \quad (1)$$

where  $D$  and  $L$  are the tubing diameter and length (in cm). The conductance of a given tube limits the nominal pumping speed by the following equation:

$$1/S_{\text{eff}} = (1/S) + (1/C_p) \text{ s/l}, \quad (2)$$

where  $S$  and  $S_{\text{eff}}$  are the nominal and effective pumping speeds. From Eq. (1) it is obvious that the furnace tube is conductance limited having a maximum conductance of  $\approx 0.015$  l/s. To summarize the rest of Fig. 1, the electrode chamber tubing has a conductance of 16 l/s and the side tubing of 4 l/s. Factoring in the 80-l/s speed of the turbomolecular pump, which is connected to the UHV system by 50-l/s tubing, results in the electrode chamber pumping at an  $S_{\text{eff}}$  of 10.5 l/s and the specimen chamber pumping at 3.5 l/s.

The above analysis treated each chamber as a separate entity; however, the turbo pump must simultaneously evacuate both chambers. To treat the furnace system as a whole the conductances must be combined. Given the law of conductances and assuming that the furnace tube effectively isolates each vacuum chamber, then total conductance is

$$C_T = \left(\frac{1}{30} + 1/(16 + 4)\right)^{-1} \text{ l/s} \quad (3)$$

or a  $C_T$  of 14 l/s. Combining with Eq. (2) results in an  $S_{\text{eff}}$  of  $\approx 12$  l/s. This value represents the tradeoff between adequate conductance and overall expense. For example, the conductance could have been increased by use of larger diameter tubing; however, then the total cost of the furnace system would have been prohibitively high. It is important to note that the turbo pump is located at the bottom of the vacuum system and thus the specimen collection chamber, located at the top, is not effectively pumped. To alleviate this problem a 20-l/s triode ion pump is attached to the specimen chamber to pump this chamber and the transfer system.

It should be recalled at this point that the dimensions of the furnace tube are dictated by the need to maintain proper gas flow during the sintering process. The obvious drawback to this design strategy is that the furnace tube could not ever be adequately pumped to UHV regardless of how large a pump is used. Such a result stems from considering the total outgassing rate of the vacuum chamber walls. For example, the ultimate pressure of a vacuum system  $P_u$  is determined by the ratio of the total outgassing rate  $Q$  to the effective pumping speed  $S_{\text{eff}}$ .

$$P_u = Q/S_{\text{eff}} \text{ Pa}, \quad (4)$$

where the typical value of  $Q$  for "clean" stainless steel is  $\approx 10^{-8}$  l Pa/s; the value for sintered alumina is higher. Considering that the furnace tube pumps at an  $S_{\text{eff}}$  of 0.015 l/s, the ultimate pressure attainable would be  $8 \times 10^{-7}$  Pa if it were made of stainless steel. Baking the furnace tube at high temperatures (1400 °C) can improve the situation.

However, the porous nature of alumina surfaces will limit the overall  $Q$  improvement.

Another complicating factor in the conductance analysis of the furnace system is the total surface area to be pumped. The standard rule of thumb in UHV is that for every 100 cm<sup>2</sup> of steel surface area, one needs to supply at least 1 l/s of effective pumping speed. The total of 6300 cm<sup>2</sup> needs to be pumped at an  $S_{\text{eff}}$  of 63 l/s; however, the conductance limitations imposed by the design constraints only provides for 12 l/s. In addition, the turbo pump, even though it has a pumping speed of 80 l/s, also has a base pressure of  $2 \times 10^{-7}$  Pa below which the pump begins to backstream. When one considers these limiting factors on the vacuum performance of the furnace system, it is not surprising that the best vacuum attained in the electrode chamber has been  $\approx 4 \times 10^{-7}$  Pa.

#### IV. THE FURNACE VACUUM SYSTEM

As mentioned above, the large furnace chamber is pumped by a trapped rotary pump (3.3 l/s) and can be isolated from the UHV system by a gate valve. To minimize any pressure differential between the furnace chamber and the UHV system, the chambers are initially pumped down simultaneously by the rotary pump. In the presence of a pressure difference, the welded bellows above the furnace would either expand or contract stressing the fragile alumina tube, or Kovar seals, resulting in mechanical failure. Once the chambers have achieved pressures lower than 10 Pa, the chambers are isolated by the furnace gate valve and the turbo and ion pumps bring the UHV system to its ultimate vacuum while the rotary pump maintains the furnace chamber at 1 Pa. As mentioned before, the 80-l/s turbo pump is located at the bottom of the vacuum system and the 20-l/s triode ion pump is attached at the top. Both pumps can be isolated from the UHV system by gate valves.

Even with both the turbo and ion pumps the furnace tube remains conductance limited in its pumping speed. This is not a major problem though because during the bakeout of the system the furnace tube is heated to  $\approx 1400$  °C. That is, the furnace must be run hotter during a bake than during particle production and sintering to ensure its cleanliness. The resulting temperature gradient between the furnace tube and the adjoining chambers (baking at  $\approx 150$  °C) is large enough to drive impurities, such as water vapor and hydrocarbons, out of the furnace tube. Once in the larger chambers, the impurities can be effectively pumped away. The result is that once UHV has been attained, the furnace tube can reach 1000 °C before there is a large pressure rise (outgassing) in the vacuum chambers. Actually, as the furnace is heated up there is a pressure burst at 200 °C, but then the total pressure in the system decreases as the furnace temperature continues to climb until 1000 °C is reached; i.e., the pressure rises from  $5 \times 10^{-7}$  to  $2 \times 10^{-6}$  Pa at 1000 °C.

## V. PARTICLE PRODUCTION PROCEDURE

The method of producing the alumina UFPs, as mentioned before, is an arc discharge between two high-purity aluminum electrodes in an oxidizing atmosphere. The following procedure is currently used to produce the UFPs: First we attain UHV in the vacuum system and then, in UHV, the furnace is heated to the desired temperature slowly over approximately 2–3 h. During the heating process the vacuum level and gas species are monitored by a mass spectrometer to ensure the cleanliness of the system. Once the furnace has stabilized, both the furnace chamber and the UHV chambers are backfilled, isolated but in conjunction, with forming and oxidizing gases, respectively. The introduction of these gases cools the furnace temperature and the power to the furnace is increased to maintain the proper setting. Once the required pressure is attained, about 6 kPa, the oxidizing gas is forced to flow up the furnace tube at the desired flow rate (which determines the particles residence time in the furnace) and exits the system through a molecular sieve and liquid-nitrogen-trapped (LN<sub>2</sub>) rotary pump. After both the furnace temperature and the gas flow have reached steady state, the arc discharge can be started and the specimen cartridge brought into the rising gas/particle stream for collection.

The arc is typically run for about 3–4 min after which the specimen is retracted into the PTS, the length of collection being governed by the number of smoke bursts in the arcing process to give a good particle density on the grid. The furnace and UHV chambers are then rough pumped simultaneously down to about 10 Pa, all the while maintaining pressure equilibrium across the welded bellows and isolation between the furnace and UHV chambers. At this vacuum level the rotary pump is isolated and the turbo and ion pumps take over to bring the UHV chambers into the  $5 \times 10^{-6}$ -Pa range, which requires 1 h. A full bake of the system will give UHV; however, this process takes about 12 h and may not be as crucial to the cleanliness of the particle surfaces. What is important, however, is that the UFPs avoid contamination from rotary pump oil and the atmosphere. After this pumpdown interval, the PTS is isolated by its gate valve. The PTS is then detached from the collection chamber and, under vacuum, transferred to the UHV-H9000 microscope by means of the custom-made grabber mechanism on the specimen transfer chamber (STC) described elsewhere.<sup>14</sup>

## VI. DISCUSSION

Figure 5 shows a typical example of the UFPs produced by the arc discharge and collected by specimen cartridge. Here the particle size distribution and the faceted nature of the particle surfaces is evident. These particles were formed in an oxidizing atmosphere of Ar-20% O<sub>2</sub> at a total pressure of 6 kPa. When the furnace is energized, sintering processes begin to occur and necks are formed between particles as arrowed. The details of the sintering process which occur in these UFPs and the atomic structure of the interfaces formed is described elsewhere.<sup>15,16</sup>

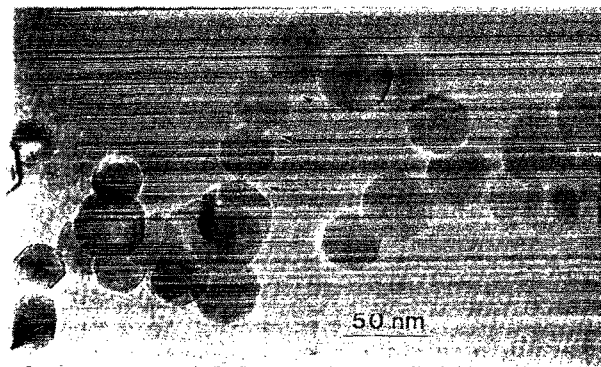


FIG. 5. Typical particle sample produced by the arc discharge method. Here the particle size distribution and the faceted nature of the particle surfaces can be discerned. The particles were produced at a pressure of 6 kPa Ar-20%O<sub>2</sub>. When the particles pass through the furnace at elevated temperatures, sintering processes occur and necks begin to grow in between the particles (arrowed). Note the evidence of surface roughening due to the high sintering temperature of  $\approx 1400$  °C.

It is appropriate at this point to mention that the hardware of the furnace system can be improved to alleviate vacuum difficulties. For example, the furnace tube can be upgraded to a larger inner diameter (e.g., 1 cm) to provide for a higher conductance for the vacuum system. An added benefit is that a larger tube has a wider range of flow rates and also is more structurally robust with respect to mechanical and thermal stresses. Along these lines, the entire furnace system plumbing can be upscaled to larger diameter tubing. That is, the current 3.8-cm-i.d. (7-cm flange o.d.) tubing can be replaced with 6.4-cm-i.d. (11.4-cm flanges) or even 10-cm-i.d. (15-cm flanges) tubing to increase the conductance of the system. Furthermore, the turbo pump should be replaced with a tandem design which has an ultimate vacuum in the  $10^{-9}$  Pa range. It should be noted, though, that such improvements represent a substantial increase in the total system cost.

The UHV furnace presented here represents a unique system that combines the particle formation, sintering, and collection processes into an integrated unit, with the advantage that these processes occur in a clean environment avoiding unwanted contaminating species. The furnace has a base pressure of  $4 \times 10^{-7}$  Pa achieved with the use of turbomolecular and ion pumps. This UHV furnace system works well, and provides the capability to expand beyond the current scope of investigation. For example, the effects of additives, or dopants, on the sintering behavior of the UFPs can be accommodated simply by alloying the proper electrode composition, i.e., magnesium can be added to the aluminum to study the role of magnesia on sintering. Furthermore, the UHV furnace system is quite versatile so that other materials can be investigated. The arc discharge apparatus is designed so that the electrode materials are easily changed; thus we can examine the structure/properties of materials such as NiO. Or, if needed, the electrodes can be swapped for a conventional "boat" configuration for standard evaporation techniques to study materials such as TiO<sub>2</sub>, etc.

## ACKNOWLEDGMENTS

The authors thank the Department of Energy (Grant No. DE-FG02-87ER45309) for the financial support of this project.

<sup>1</sup>J. Karch, R. Birringer, and H. Gleiter, *Nature* **330**, 556 (1987).

<sup>2</sup>A. H. Chokshi, A. Rosen, J. Karch, and H. Gleiter, *Scr. Metall.* **23**, 1679 (1989).

<sup>3</sup>G. W. Nieman, J. R. Weertman, and R. W. Seigel, *Scr. Metall.* **23**, 2013 (1989).

<sup>4</sup>G. W. Nieman, J. R. Weertman, and R. W. Seigel, *Scr. Metall.* **24**, 145 (1990).

<sup>5</sup>G. W. Nieman, J. R. Weertman, and R. W. Seigel, *J. Mater. Res.* **6**, 1012 (1991).

<sup>6</sup>E. O. Hall, *Proc. Phys. Soc. London, Sect. B* **64**, 747 (1951).

<sup>7</sup>N. J. Petch, *J. Iron Steel Inst.* **174**, 25 (1953).

<sup>8</sup>G. A. Somorjai, in *Fundamental Topics in Physical Chemistry*, edited by H. S. Johnston (Prentice-Hall, Englewoods Cliffs, NJ, 1972), Vol. 3.

<sup>9</sup>A. Howie and L. D. Marks, *Philos. Mag. A* **49**, 95 (1984).

<sup>10</sup>J. E. Bonevich and L. D. Marks, *Ultramicroscopy* **35**, 161 (1991).

<sup>11</sup>S. Iijima, *Jpn. J. Appl. Phys.* **23**, L347 (1984).

<sup>12</sup>C. E. Warble, *J. Mater. Sci.* **20**, 2512 (1985).

<sup>13</sup>M. Morgan, Ability Engineering, 16140 Vincennes Avenue, S. Holland, IL 60473.

<sup>14</sup>J. E. Bonevich and L. D. Marks, *Hitachi Instrument News* **17**, 4 (1989).

<sup>15</sup>J. E. Bonevich, Ph.D. dissertation, Northwestern University, 1991.

<sup>16</sup>J. E. Bonevich and L. D. Marks (unpublished).